Zincblende and wurtzite phases in InN epilayers and their respective band transitions

P. Specht[a,b,*], J.C. Ho[a,b], X. Xu[a,b], R. Armitage[a,b], E.R. Weber[a,b], E. Erni[c,1], C. Kisielowski[d]

[a]*Lawrence Berkeley National Laboratory, Materials Sciences Division, Berkeley, CA, USA*
[b]*Materials Science and Engineering Department, University of California, Berkeley, CA 94720, USA*
[c]*Department of Chemical Engineering and Material Science, University of California, Davis, CA 95616, USA*
[d]*National Center for Electron Microscopy, LBNL, One Cyclotron Road, Berkeley, CA, USA*

Available online 23 January 2006

Abstract

Zincblende and wurtzite phases of InN are found in InN epilayers deposited by molecular beam epitaxy on GaN buffers which were grown by metal organic chemical vapor deposition. Valence electron energy loss spectroscopy (VEELS) was applied to determine band transitions in both phases of InN. GaN buffer layers were used as VEELS reference. The chemistry and crystalline structure of the observed areas was recorded simultaneously to exclude a contribution from oxides and/or metal clusters or extended defects such as grain boundaries. At room temperature a band transition for wurtzite InN was found at (1.7 ± 0.2) eV and for zincblende InN at (1.4 ± 0.2) eV that are ascribed to the fundamental bandgaps of the respective polytypes. Those values correlate well with recent results of various research groups measuring the bandgap in InGaN alloys with VEELS.
Published by Elsevier B.V.

Keywords: A1. Band transitions; A1. Characterization; A1. VEELS; B1. Nitrides; B1. Polytypes

1. Introduction

The InGaN alloy system is of great scientific and technological interest as it provides for a variety of novel opto-electronic and high-power electronic device applications such as all-color light emitting diodes, ultrahigh efficient solar cells or high electron mobility transistors. Challenges which have yet to be overcome include strain engineering, heat dissipation, general device reliability and aging effects. While the Ga-rich area of this alloy system is fairly well understood there is still controversy about the physics behind the known material properties in InN and In-rich InGaN alloys.

This paper focuses on local crystallographic identification and band transition measurements of InN in a transmission electron microscope (TEM). This method was chosen to exclude the effect of grain boundaries,

(metal) inclusions and additional phases such as oxides which may largely affect the InN properties such as the material's optical absorption and/or photoluminescence. These optical measurements require modelling for the interpretation of the data which can be challenging in cases where a large defect concentration is involved. For example, it was found in low-temperature grown GaAs (LT-GaAs) which contains high concentrations of arsenic antisite defects that the optical properties can be dominated by the crystal defects rather than the host material itself. In particular, photoluminescence spectra (see for example Ref. [1]) and optical absorption spectra (see for example Ref. [2]) can be dominated by defect bands. Both optical methods were repeatedly used to determine the fundamental bandgap of InN (for example Refs. [3,4]) which also contains defects in large concentrations.

2. Experimental procedure

Here, the choice of experiment for the determination of band transitions in InN epilayers is scanning transmission electron microscopy (STEM). Epilayers were imaged in a

---

*Corresponding author. Department of Materials Science and Engineering, UC Berkeley, CA, USA.

E-mail address: specht@socrates.berkeley.edu (P. Specht).
[1]Now at FEI Electron Optics, 5600 KA Eindhoven, The Netherlands.

200 keV FEI TECNAI G^2 microscope with a monochromated nanoprobe beam which allows for a local investigation with an electron beam of 2 nm diameter and an energy resolution better than 200 meV. This microscope is located at the National Center for Electron Microscopy at the Lawrence Berkeley National Laboratory, CA. Band transitions in InN were measured by valence electron energy loss spectroscopy (VEELS) and compared to band transitions in hexagonal GaN, that was used as a standard for comparison.

VEELS probes the combined density of states of the band structure [5]. There are no reports about a dependence of the signal on the Fermi level. In contrast, such a dependence would be unexpected since energy losses occur locally under high-injection conditions that make a description of band occupation in terms of a Fermi level meaningless. Such a view is supported by bandgap measurements in many semiconductors such as GaAs, diamond, silicon or various oxides [5] that so far did not show indications of a Fermi-level dependent signal.

In TEM electron beam damage is always of concern and typically addressed by short-time exposure and signal reproduction. The most common signal distortion in VEELS comes from local hydrocarbon deposition that degenerates the signal. Such effects can be visualized by imaging and were found to be of no relevance here since the signal is well reproducible.

The InN epilayers were deposited onto a (0 0 0 1) GaN buffer, grown by metal organic chemical vapor deposition (MOCVD) on (0 0 0 1) sapphire. A typical InN epilayer thickness is 800–1000 nm, and the deposition was done under In-rich flux conditions. Further details of the epilayer growth are described elsewhere [6]. The epilayers' oxygen concentration is high, about $10^{20}/cm^3$. Any oxide phases can clearly be distinguished from the InN matrix in the TEM analysis and are not included in this study. The oxygen distribution in the InN epilayers will be published elsewhere [7].

X-ray diffraction analysis was performed in a Siemens diffractometer with a 4-Ge-crystal monochromator. Lattice constants were determined from interplanar distances. Those crystallographic plane distances were extrapolated from [0 0 0 2], [0 0 0 4], [0 0 0 6] and [1 0 $\bar{1}$ 2], [2 0 $\bar{2}$ 4] normal coupled scans utilizing the following equation [8]

$$c_h = c_{\text{real}} \times (1 - D/L \times p_h)$$
$$\text{with } p_h = \cos^2(\Theta)/\sin(\Theta), \quad (1)$$

$$c_h = h\lambda/(2\sin(\Theta)),$$

where D is the sample deviation from eucentric height, L the sample distance to radiation source, $h = 2, 4, 6$ for [0 0 h] reflections, c_{real}: extrapolated interplanar distance.

TEM samples were prepared in cross-sectional geometry by Ar ion milling and—in some cases—a final etching step to minimize surface roughness [9]. The VEELS measurements were performed with a monochromated FEI Tecnai

G^2 STEM/TEM as described above. GaN buffer layers were investigated to provide a reference signal that was extensively studied before (see for example Refs. [10,11]). VEELS measurements were accompanied by high-resolution TEM to determine the crystal structure of the epilayers and to identify other phases if present. VEELS spectra were only taken from areas identified as wurtzite InN, zinc-blende InN or wurtzite GaN, with no other crystal phases, especially no oxides or indium metal clusters, present.

3. Results and discussion

A large deviation of the c lattice constant was observed earlier in InN epilayers grown on MOCVD GaN buffers [6]. The corresponding strain in the epilayer was mainly attributed to a uni-axial stress as it occurs when defects are incorporated site specifically along (0 0 0 1) crystallographic planes. Fig. 1 shows the high-resolution X-ray diffraction
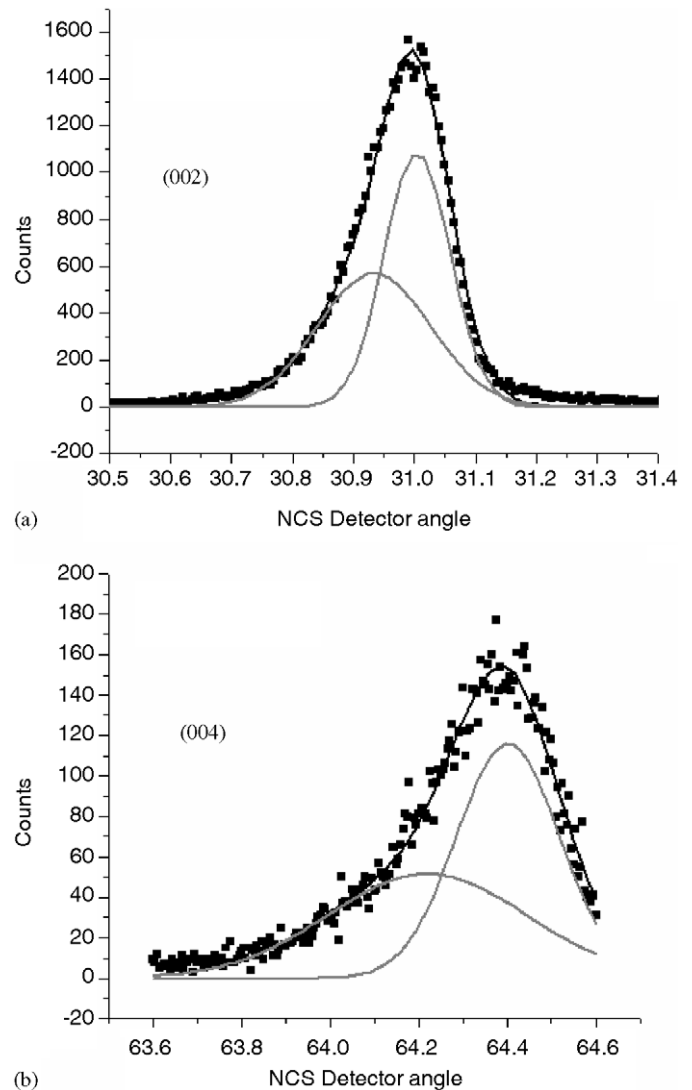

Fig. 1. X-ray normal coupled scan of InN epilayer deposited on MOCVD GaN buffer, the solid lines are fitted Gaussian functions (gray: single peaks, black: superposition of two peaks).

of (0 0 0 2) and (0 0 0 4) reflections of InN (rocking curves) which clearly show a second peak appearing in the overall asymmetric diffraction peak. The second peak was found to correlate with (1 1 1)-type crystallographic planes of the zincblende phase of InN. The corresponding lattice parameters from the complete X-ray diffraction analysis are given in Table 1. For details on the lattice parameter evaluation see Ref. [6]. It should be noted that the presence of polytypes of InN does not explain the observed uni-axial stress response in the epilayer. Preferential incorporation of point defects along (0 0 0 1) or (1 1 1) planes may have caused the strain in both crystallographic phases, wurtzite and zincblende InN, respectively, preferentially incorporated oxide platelets were not found.

In a TEM the polytypes of InN were confirmed. In thin TEM sample areas those phases can be investigated separately. Fig. 2 shows such an area with wurtzite and zincblende InN. Power spectra taken from local image areas allow for their identification as shown by the insets. The local VEELS measurements were performed after

identification of the respective phase of the investigated grains.

VEELS, also called "low-loss EELS", is an established method to measure band transitions in a variety of materials. First, high-bandgap materials such as BN, MgO or diamond were the subject of VEELS investigations but also the band transitions of semiconductors such as GaAs were measured [5]. Recently, the development of monochromated electron beams, which narrow the zero loss, became available. This advanced technology provides an energy resolution smaller than 200 meV and therefore gives access to measuring narrow gap semiconductors as well. For wurtzite phase InGaN alloys, including InN various VEELS measurements were published recently [10–14].

Table 1
Lattice constant evaluation for wurtzite InN with zincblende phase inclusions

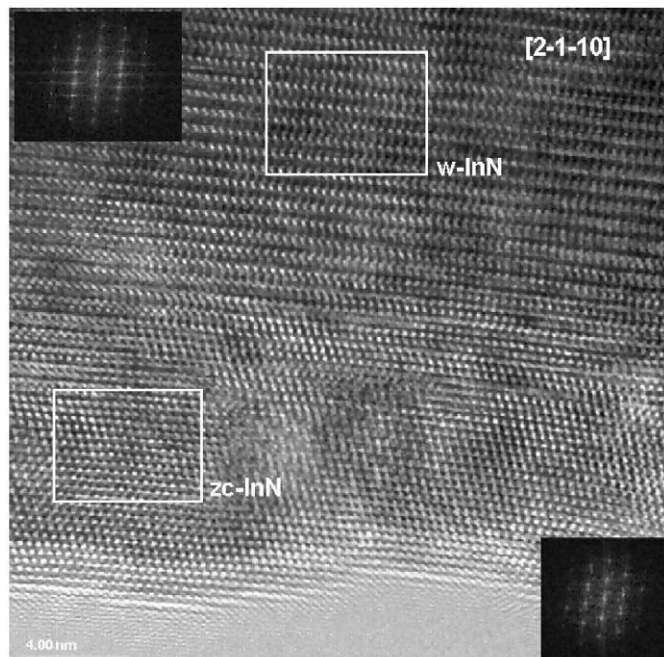|	Theoretical (x)	Single peak	Double peak	Mismatch (%)
a_wurtzite (nm)	0.3545	0.3534	0.3535	0.31/0.28
c_wurtzite (nm)	0.5703	0.5804	0.5799	1.77/1.68
a_zincblende (nm)	0.498		0.5035	1.10

Fig. 2. High-resolution TEM image of an InN epilayer with zincblende and wurtzite type areas, insets show the corresponding diffraction patterns of wurtzite and zincblende InN.
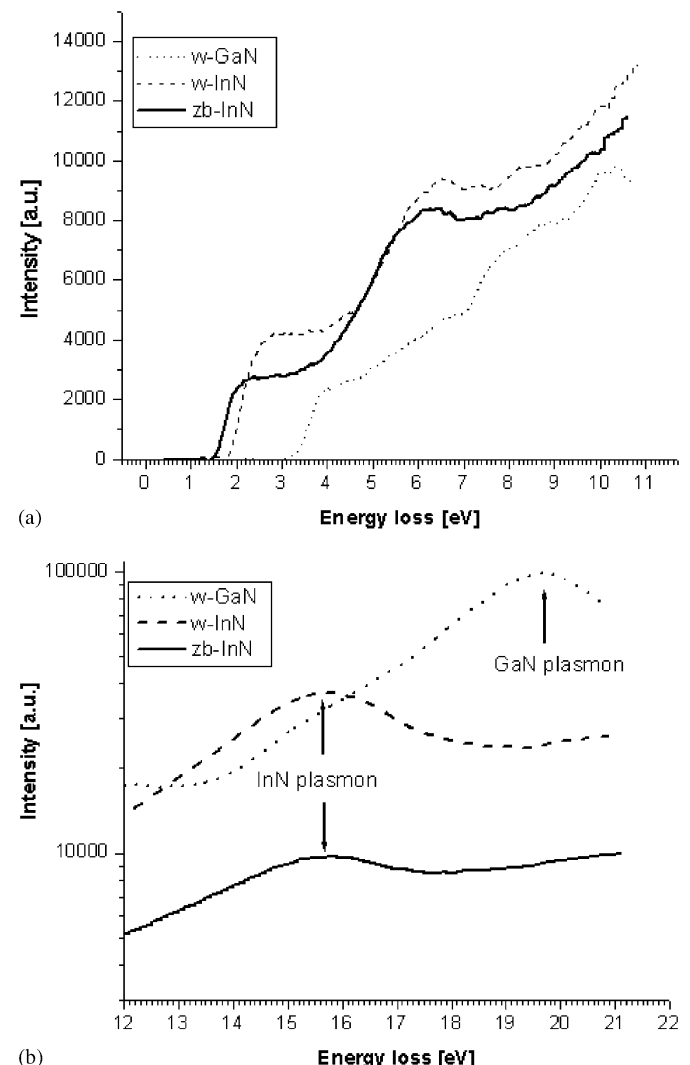

Fig. 3. Typical VEELS spectra of wurtzite GaN (dotted line), wurtzite InN (dashed line) and zincblende InN (solid line), the background is removed, (a) onset of first observed energy loss shows the bandgap of the respective materials, (b) plasmon peaks are observed at 19.5 eV for GaN, 15.7 eV for InN, the latter peak energy is identical for wurtzite and zincblende phases.

Fig. 3 shows typical VEELS spectra of a GaN buffer layer (dotted line), a wurtzite InN area (dashed line) and a zincblende InN area (solid line). The VEELS spectra are shown with the background removed (no zero loss). At higher energies of the spectra (Fig. 3b) the plasmon peak can be observed which is characteristic for the host material, at (19.5 ± 0.1) eV for GaN and (15.7 ± 0.1) eV for InN, and at the same position for wurtzite and zincblende InN. The plasmon peak position also confirms that InN is measured and not another crystallographic phase such as indium-oxide. As can be clearly seen (Fig. 3a) no significant energy loss is observed below 1 eV; the first band transition in GaN is found at about 3.3 eV while the first band transition in wurtzite InN is observed at about 1.8 eV. In zincblende InN the first band transition is found at about 1.5 eV (all Fig. 3a). The observation of a slightly lower bandgap for zincblende InN than for wurtzite InN is consistent with bandgap measurements of the polytypes in GaN and AlN (see for example Ref. [15]). The bandgap energy determined by VEELS is a room temperature value due to a slight local temperature increase in the TEM specimen (see also Refs. [13,14]). The bandgap value for GaN agrees well with literature data (see for example Ref. [15]).

The band transitions in zincblende InN were investigated at several areas of the TEM samples. Fig. 4 shows the first derivative of typical VEELS spectra for zincblende InN, the original spectra are given in the inset of Fig. 4. The first derivative of the processed signal can be described by a superposition of Lorentz functions (smooth curves in Fig. 4) within the experimental noise. This fitting procedure was utilized to characterize the various band transitions by their inflection points as suggested previously by Lazar et al. [10]. We prefer this description over the commonly used bandgap determination by a power law (PL) $(E - E_g)^{0.5}$, see

for example Ref. [11], that is more suitable if no signal overlap occurs. Using the full-width and half-maximum (FWHM) of the respective peaks in the derivative plot one can link both methods, inflection point (IP) and PL, and determine the bandgap E_G [13]

$$E_G = E_{PL} \approx E_{IP} - 0.5 \times \text{FWHM}. \qquad (2)$$

Band transition values given in this paper include this correction or refer directly to E_{PL}.

In Fig. 4 it is clearly visible that the first strong peak in the derivative energy spectra ($\Delta I / \Delta E$ versus E) is located at an energy of about 1.6 eV. All recorded VEELS spectra for zincblende InN have similar features than the two shown in Figs. 3 and 4. This corresponds to a corrected (room temperature) bandgap energy of (1.4 ± 0.2) eV. Also, a multitude of different spectra were taken from various areas of different InN epilayers, for wurtzite InN the bandgap energy was always similar to the one shown in Fig. 3 and was determined to (1.7 ± 0.2) eV [13]. A variation of the bandgap energy was never observed, neither for epilayers with vastly different conductivity—absorption edge energies vary in those epilayers from 0.8 to 1.5 eV— nor for TEM specimen areas with different thicknesses as would be expected if the VEELS measurements were dominated by the epilayer's surface conditions. In zincblende InN higher energy band transitions are still to be determined, only a rather broad second peak around (4.2 ± 0.8) eV was found, which is likely composed of various band transitions. Those transitions will have to be investigated in more detail in future when epilayers of higher crystalline quality are available (less noise in the VEELS spectra).

The currently available VEELS bandgap energies for $In_xGa_{1-x}N$, $x > 0$, are all in clear discrepancy to the recently published data obtained by photoluminescence and optical absorption [3,4,16,17]. However, earlier publications [18,19] correlate well with the VEELS results. Fig. 5 gives a summary of various prior published bandgap
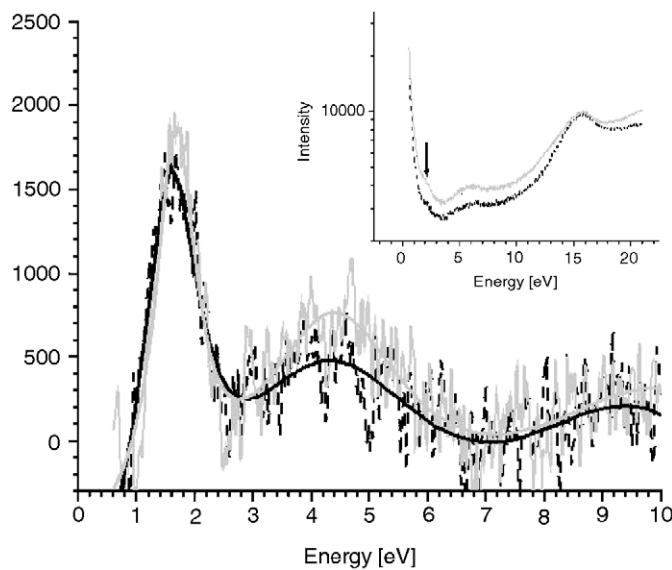

Fig. 4. First derivatives of the electron energy loss spectra of zincblende InN, the inset shows the original spectra.
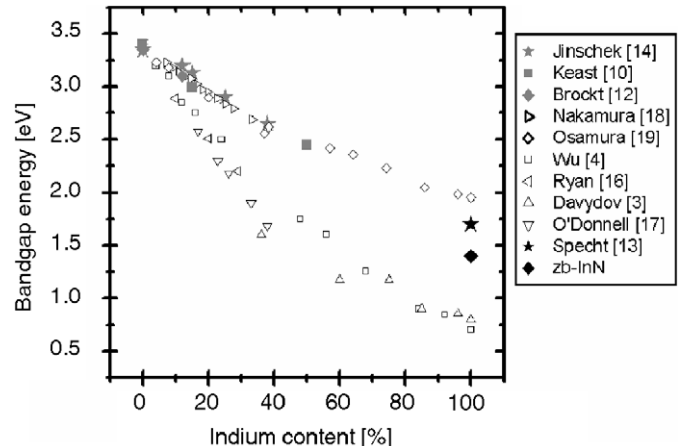

Fig. 5. Selected bandgap energy measurements for the InGaN alloy system (see also Ref. [14]). Included are recent VEELS results (filled symbols).

data, VEELS data are given in solid symbols, PL and optical absorption energies in open symbols. It is found that the bandgap energies as measured by VEELS depend almost linearly on the indium concentration x in $In_xGa_{1-x}N$ alloys. The systematic deviation of PL and absorption edge energies from the bandgap as measured by VEELS is not restricted to InN but extends to the whole InGaN alloy system. It is interesting that InGaN epilayers produced approximately 10 years ago show no significant deviation between the bandgap energies determined by the different methods.

As a first hypothesis it is assumed that the progressing development of $In_xGa_{1-x}N$ alloys resulted in the formation of local inhomogeneities such as In-rich clusters as were found in Ref. [14]. Consequently, if those clusters are the dominant sources for optical transitions, the bandgap of their composition will be measured by PL. As those clusters have a higher concentration of indium than the average indium content in the epilayers (usually measured by X-ray diffraction) lower "effective" bandgap energies are recently measured for those materials while local composition variations are detected in a VEELS analysis which facilitates a correct bandgap determination. Although this does describe the energy variation in InGaN alloys with In concentrations lower than 40% (more than 60% Ga), the origin of the 0.8 eV photoluminescence energy in InN remains unclear.

4. Conclusions

In conclusion, band transitions in wurtzite and zincblende InN grown by molecular beam epitaxy were observed utilizing VEELS. The respective polytypes of indium-nitride were identified utilizing the energy position of the plasmon peak and the power spectra of the investigated areas. A dominant energy transition is observed for wurtzite InN at approximately (1.7 ± 0.2) and (1.4 ± 0.2) eV for zincblende InN which are ascribed to the fundamental bandgaps of the respective InN phases at approximately room temperature. The measured bandgap energy for wurtzite InN correlates well with recently published VEELS data of wurtzite InGaN with indium concentrations lower than 40% and an almost linear bandgap energy function is observed.

References

[1] M. Tajima, H. Tanino, K. Ishida, in: H.J. von Bardeleben (Ed.), Proceedings of the 14th International Conference on Defects in Semiconductors, Trans. Tech. Publ. Ltd., Aedermannsdorf, 1986, pp. 1265.
[2] G.M. Martin, Appl. Phys. Lett. 39 (1981) 747.
[3] V.Yu. Davydov, A.A. Klochikhin, R.P. Seisyan, V.V. Emtsev, et al., Phys. Stat. Solidi b 229 (2002) R1.
[4] J. Wu, W. Walukiewicz, K.M. Yu, J.W. Ager III, E.E. Haller, H. Lu, W.J. Schaff, Y. Saito, Y. Nanishi, Appl. Phys. Lett. 80 (2002) 3967.
[5] B. Rafferty, L.M. Brown, Phys. Rev. B 58 (1998) 10326.
[6] P. Specht, R. Armitage, J. Ho, E. Gunawan, Q. Yang, X. Xu, C. Kisielowski, E.R. Weber, J. Crystal Growth 269 (2004) 111.
[7] X. Xu, P. Specht, R. Armitage, J.C. Ho, C. Kisielowski, E.R. Weber, Appl. Phys. Lett. 87 (2005) 092102.
[8] V.S. Harutyunyan, A.P. Arivazyan, E.R. Weber, Y. Kim, Y. Park, S.G. Subramanya, J. Phys. D 34 (2001) A35.
[9] C. Kisielowski, Z. Liliental-Weber, S. Nakamura, Jpn J. Appl. Phys. 36 (1997) 6932.
[10] S. Lazar, G.A. Botton, M.-Y. Wu, F.D. Tichelaar, H.W. Zandbergen, Ultramicroscopy 96 (2003) 535.
[11] V.J. Keast, A.J. Scott, M.J. Kappers, C.T. Foxon, C.J. Humphreys, Phys. Rev. B 66 (2002) 125319.
[12] G. Brockt, H. Lakner, Micron. 31 (2002) 435.
[13] P. Specht, J.C. Ho, X. Xu, R. Armitage, E.R. Weber, R. Erni, C. Kisielowski, Solid State Commun. 135 (2005) 340.
[14] J.R. Jinschek, R. Erni, N.F. Gardner, A.Y. Kim, C. Kisielowski, Solid State Commun. (2005), in press, available online 21 November 2005.
[15] I. Vurgaftman, J.R. Meyer, J. Appl. Phys. 94 (2003) 3675.
[16] P. Ryan, C. Mc Guinness, J.E. Downes, K.E. Smith, Phys. Rev. B 65 (2002) 205201.
[17] K.P. O'Donnell, J.F.W. Mosselmans, R.W. Martin, S. Pereira, M.E. White, J. Phys: Condens. Matter 13 (2001) 6977.
[18] S. Nakamura, J. Vac. Sci. Technol. A 13 (1995) 705.
[19] K. Osamura, S. Naka, Y. Murakami, J. Appl. Phys. 46 (1975) 3432.